

Fe/Au Galvanic Nanocells to Generate Self-Sustained Fenton Reactions Without Additives at Neutral pH

Gubakhanim Shahnazarova,^{[a],[b]} Nour Al Hoda Al Bast,^{[a],[b]} Jessica C. Ramirez,^{[a],[b]} Josep Nogues,^{[a],[c]} Jaume Esteve,^[d] Jordi Fraxedas,^[a] Albert Serra^{[e],[f]}, Maria J. Esplandiu,^{*,[a]} Borja Sepulveda,^{*,[d]}

[a] Dr. Gubakhanim Shahnazarova, Nour Al Hoda Al Bast, Jessica C. Ramirez, Prof. Josep Nogues, Dr. Jordi Fraxedas, Dr. Maria J. Esplandiu
Catalan Institute of Nanoscience and Nanotechnology (ICN2), CSIC and BIST, Campus UAB, Bellaterra, E-08193 Barcelona.

Email: mariajose.esplandiu@icn2.cat

[b] Gubakhanim Shahnazarova, Nour Al Hoda Al Bast, Jessica C. Ramirez
Universitat Autònoma de Barcelona, 08193 Cerdanyola del Vallès, Barcelona, Spain.

[c] Prof. Josep Nogues
ICREA, Pg. Lluís Companys 23, 08010 Barcelona, Spain

[d] Prof. Jaume Esteve, Dr. Borja Sepulveda
Instituto de Microelectrónica de Barcelona (IMB-CNM, CSIC); Barcelona, 08193, Spain.

Email: borja.sepulveda@csic.es

[e] Dr. Albert Serra
Grup d'Electrodeposició de Capes Primes i Nanoestructures (GE-CPN), Departament de Ciència de Materials i Química Física, Universitat de Barcelona, Martí i Franquès, 1, E-08028, Barcelona, Catalonia, Spain.

[f] Dr. Albert Serra
Institute of Nanoscience and Nanotechnology (IN2UB), Universitat de Barcelona, Barcelona, Catalonia, Spain.

MATERIALS AND METHODS

1. Synthesis of large pore silica nanoparticles

The large pore silica particles (LPSNPs) with pore size around 35 nm and diameters ranging from 200 nm to 250 nm were synthesized by the Stöber method (Fig. S1). Firstly, a cetyltrimethylammonium bromide (CTAB) (1.02 mg) and water (340 mL) mixture was prepared in an Erlenmeyer flask under vigorous stirring. Subsequently, ethanol (120 mL), 30 % NH_3 , (1.5 mL), 1-3-5, Trimethylbenzene (TMB) (1.5 mL), and water (340 mL) were added to the mixture, maintaining the solution temperature at 35°C. Finally, the solution was heated to 80°C before adding tetraethyl orthosilicate (TEOS) (1 mL) dropwise. After 2 h, the particles were recovered by centrifugation (10000 rpm, 5 min), cleaned with an NH_4NO_3 /ethanol solution, and redispersed in ethanol.

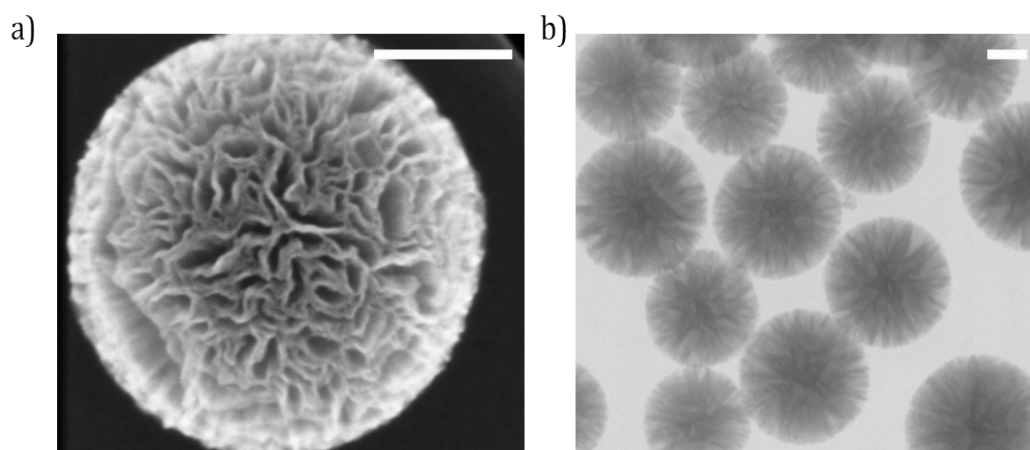


Figure S1. STEM image of the large porous silica particles. Scale bar a) 200 nm, b) 100 nm

2. Fabrication of Fe/Au galvanic nanocells to generate Fenton reactions

The Fe/Au GNCs were fabricated by combining colloidal self-assembly and physical vapor deposition techniques as shown schematically in Fig. 1a. Silicon wafers (Siegert Wafer GmbH) were used as substrates for the colloidal self-assembly of the porous silica nanoparticles. Initially, the substrate was thoroughly cleaned several times with acetone and isopropanol, then rinsed with Milli-Q water and dried with a nitrogen gun. The silicon wafer was immersed inside a water filler container and the aqueous suspension of colloidal LPSNPs was initially deposited at the liquid/air interface over the silicon wafer. Once a close-packed monolayer array of LPSNPs was formed at the air/water interface, the water was drained, thereby depositing the LPSNPs array on the silicon wafer. Then, the Si substrate with the array of LPSNP was cleaned with oxygen plasma (400 W, O_2 60 sccm) for five minutes (PS210, PVA Tepla America, Inc.) to fully remove any leftover surfactants. This process avoids the need for calcination and leaves a highly hydrophilic silica surface. Finally, the Fe (60 nm)/Au (20 nm) bilayer was deposited on the array of nanoporous SiO_2 beads using electron beam evaporation (UNIVEX 450, Leybold). Arrays in which only a Fe (60 nm) layer was deposited were used for comparison to reveal the galvanic effects.

3. Characterization of the Galvanic nanocells to generate Fenton reactions.

The morphology of the GNCs was analyzed by scanning electron microscopy (FEI Magellan 400L XHRSEM), and energy-dispersive x-ray spectroscopy (EDX) elemental mapping was monitored in the same microscope by an Oxford Instruments Ultim Extreme EDX detector system (Fig. S2).

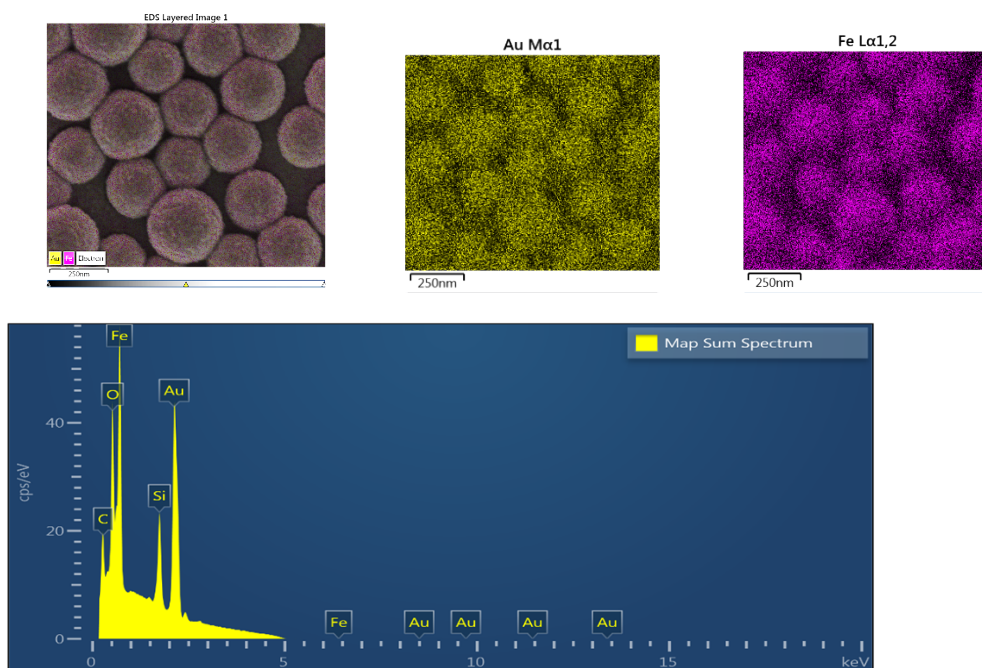


Figure S2. EDX elemental mapping of Fe/Au nanocells

Element	Atomic %
Si	17.85
Fe	51.50
Au	30.65
Total:	100.00

We also carried out high resolution SEM of the similar samples with only the deposited Fe layer to show the high roughness of the Fe layer (Fig. S3).

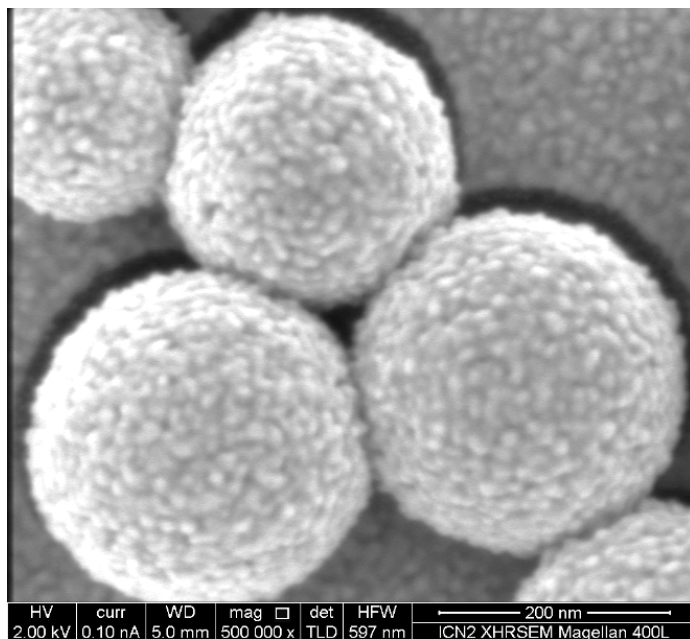


Fig. S3: High Resolution SEM image of the porous SiO₂ covered by the 60 nm thick Fe layer.

We performed TEM with EDX line scan profile to show the 3D structure and composition of the electron-beam deposited Fe and Au layers that partially cover the porous SiO₂ nanoparticles (Fig. S4 a and b), and X-ray diffraction to assess the atomic structure of the layers.

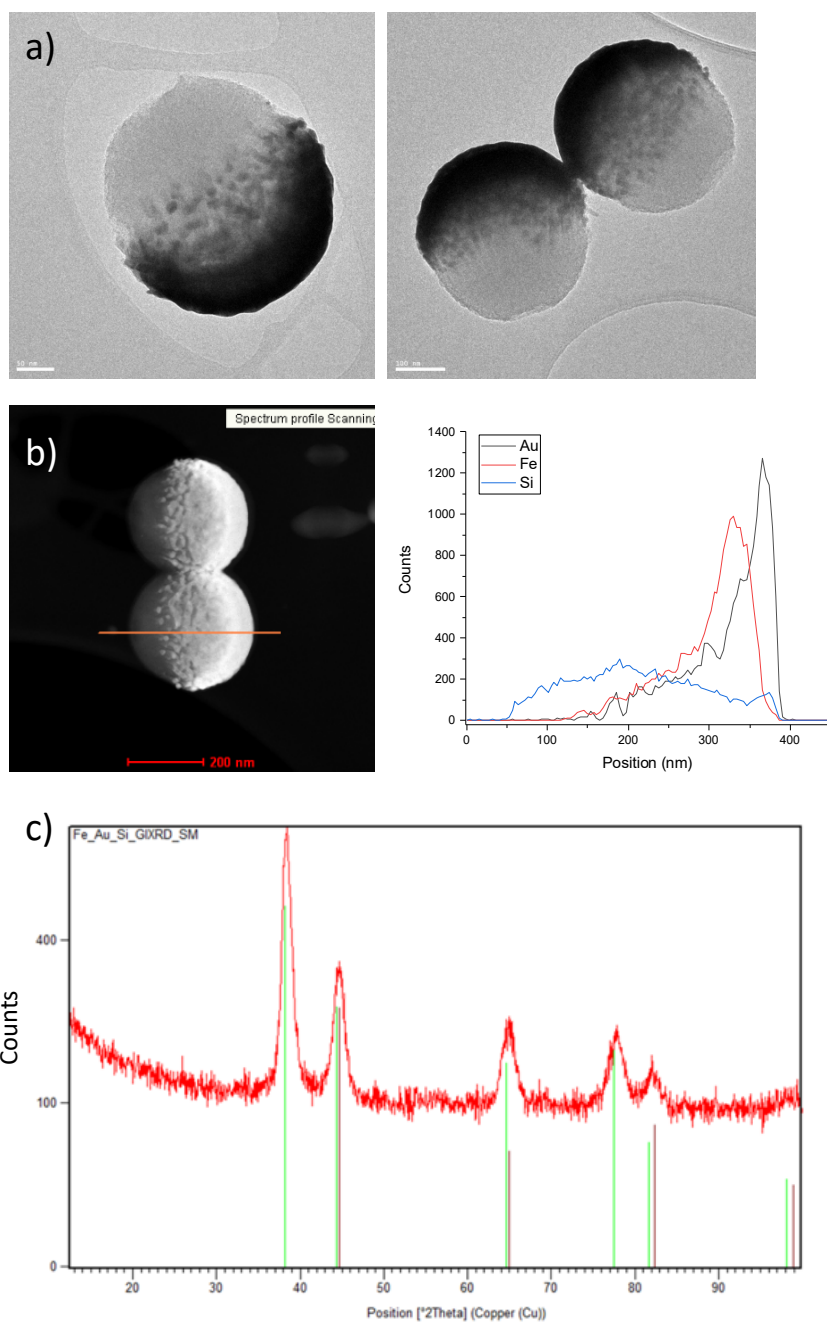


Fig. S4: a) High Resolution TEM images for the Fe 60 nm / Au 20 nm GNCs, also showing more metal nanostructuring at the rims and b) profile of the elemental composition measured across a particle through a line scan, with the particle image indicating the EDX line scan position. c) XRD pattern of the Fe/Au bilayers. The vertical bars show the position of the reflections corresponding to Au (green) and Fe (dark-red).

Detection of the produced H_2O_2

The combination of Amplex Red (10-acetyl-3,7-dihydroxyphenoxazine) and horseradish peroxidase (HRP) has been used as ultrasensitive assay to detect hydrogen peroxide (H_2O_2), with a detection limit of around 50 nM. In the presence of HRP, the Amplex Red reagent reacts with H_2O_2 in a 1:1 stoichiometry to produce the red-fluorescent oxidation product, resorufin. The concentration of H_2O_2 is proportional to the generated resorufin. The fluorescence emission

peak of resorufin is at 587 nm upon excitation at 488 nm. This process was monitored using confocal fluorescence microscopy (Leica, SP5) by focusing on the interface of the galvanic Fenton nanogenerators.

The procedure started with the preparation of fresh stock solutions: 10 mM Amplex Red reagent in dimethyl sulfoxide (DMSO), 1X Reaction Buffer, 10 U/mL HRP, and 20 mM H₂O₂ in 1X buffer. The H₂O₂ calibration curve was prepared by diluting the appropriate amount of 20 mM H₂O₂ into 1 X buffer to produce H₂O₂ concentrations of 0.5, 2.5, 5, 7.5, and 10 μM, including a no-H₂O₂ control. Appropriate amounts of Amplex red and HRP were added to the standard solutions of H₂O₂ to achieve a final concentration of 100 μM in the case of Amplex Red and 0.2 U/mL in the case of HRP. The reaction between H₂O₂, Amplex Red, and HRP was incubated to produce the resorufin, as a fluorescent probe of the H₂O₂ standard solutions. The resulting fluorescence intensity of resorufin as a function of the concentration of the standard H₂O₂ solutions is plotted in Fig. S5. Each value is the average of three fluorescence measurements. Then, the concentration of H₂O₂ at the GNCs was determined by the addition of 100 μM Amplex Red and 0.2 U/mL HRP. The produced H₂O₂ concentration was determined by fitting the linear part of the calibration plot (dashed line).

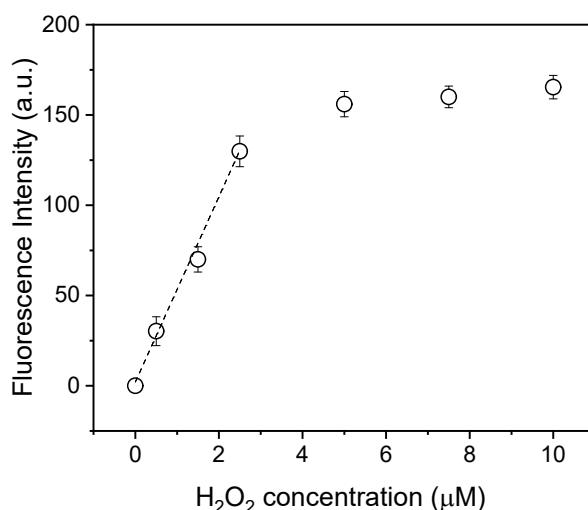


Figure S5. The calibration curve was obtained by measuring resorufin fluorescence as a function of standard solutions of H₂O₂. Background fluorescence, determined for a no-H₂O₂ control reaction, has been subtracted from each value as well as any background fluorescence from the support substrate of the Au/Fe and Fe nanostructures. The dashed line marks the linear range of the calibration.

4. Detection of the produced Fe²⁺/Fe³⁺ cations

Fingerprints of the iron ion release can be detected spectrophotometrically by measuring the absorbance of the water solution in contact with the nanostructures at different reaction times within a wavelength range of 200 to 350 nm. However, discrimination between Fe²⁺ and Fe³⁺ cannot be accomplished. To discriminate and quantify the released concentration of Fe²⁺ and Fe³⁺, a colorimetric assay selective to Fe²⁺ was used. The spectrophotometric measurements were performed with a UV-vis spectrophotometer (Cary 4000, PerkinElmer). In this assay, Fe²⁺ reacted with o-phenanthroline to form a colored complex with an absorption peak at 511 nm.

The absorption at this specific wavelength was utilized for constructing a calibration curve, employing standard Fe^{2+} solutions within the concentration range of 1.0×10^{-7} M to 1.10×10^{-4} M (Fig. S6 a and b). Hydroxylamine was added as reducing agent to the standard solutions to ensure that iron was in its 2+ oxidation state. To determine the Fe^{2+} and Fe^{3+} concentrations released by the Fe/Au and Fe nanogenerators, two aliquots of the water solution in contact with the Au/Fe and Fe nanostructured surfaces were extracted after 15 minutes of reaction. The first aliquot was complexed with o-phenanthroline and used to determine the Fe^{2+} concentration produced in the unknown sample. The second aliquot was put in contact with o-phenanthroline and the reducing agent hydroxylamine. The use of the reducing agent allowed for obtaining the total concentration of iron cations in the form of Fe^{2+} in the unknown sample. This includes the Fe^{2+} actually produced during the catalytic process and the Fe^{3+} that was produced during the catalytic process but converted into Fe^{2+} with the reducing agent. The concentration of Fe^{3+} was then obtained by subtracting the iron content of both aliquots. The total iron concentration for Au/Fe and Fe nanostructured surfaces was also obtained by Inductively Coupled Plasma Mass Spectrometry (ICP-MS) measurements at different reaction times.

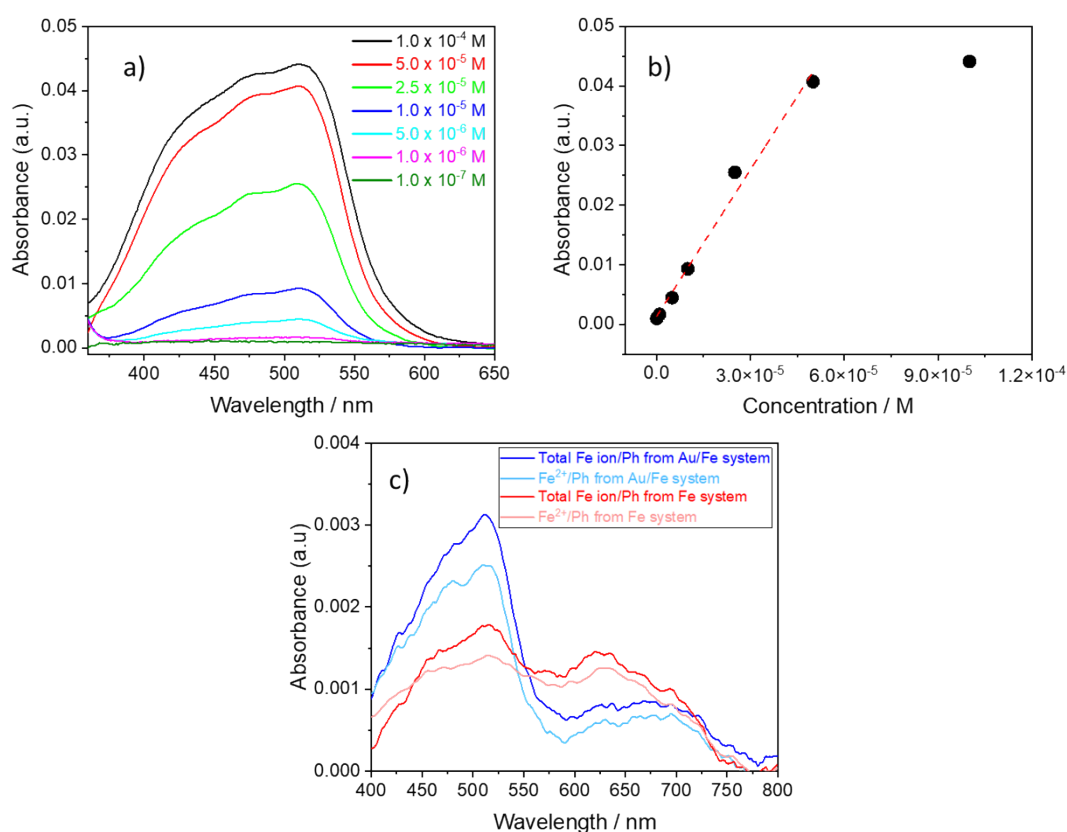


Figure S6. (a) Absorbance of the different standard Fe^{2+} concentrations as a function of the wavelength, (b) calibration curve at 511 nm (the dashed line indicates the linear range of the calibration) and (c) Absorbance of the water samples undergoing reaction with Fe/Au and Fe nanogenerators. The absorbance peaks of the aliquots of the Fe^{2+} /phenanthroline complex corresponding to the actual release of Fe^{2+} by the Au/Fe and Fe nanogenerators are depicted by light blue and light red solid lines, respectively. Additionally, the absorption curves of the Fe^{2+} /phenanthroline complex representing the total release of iron into the solution by the interaction with both nanogenerators (Au/Fe blue line and Fe red line) are displayed. As pointed

out before, these latter ones include the Fe^{3+} concentration converted into Fe^{2+} through reaction with hydroxylamine. (Ph denotes *O*-phenantroline).

5. Structural and oxidation state analysis of the samples before and after the galvanic reaction in water

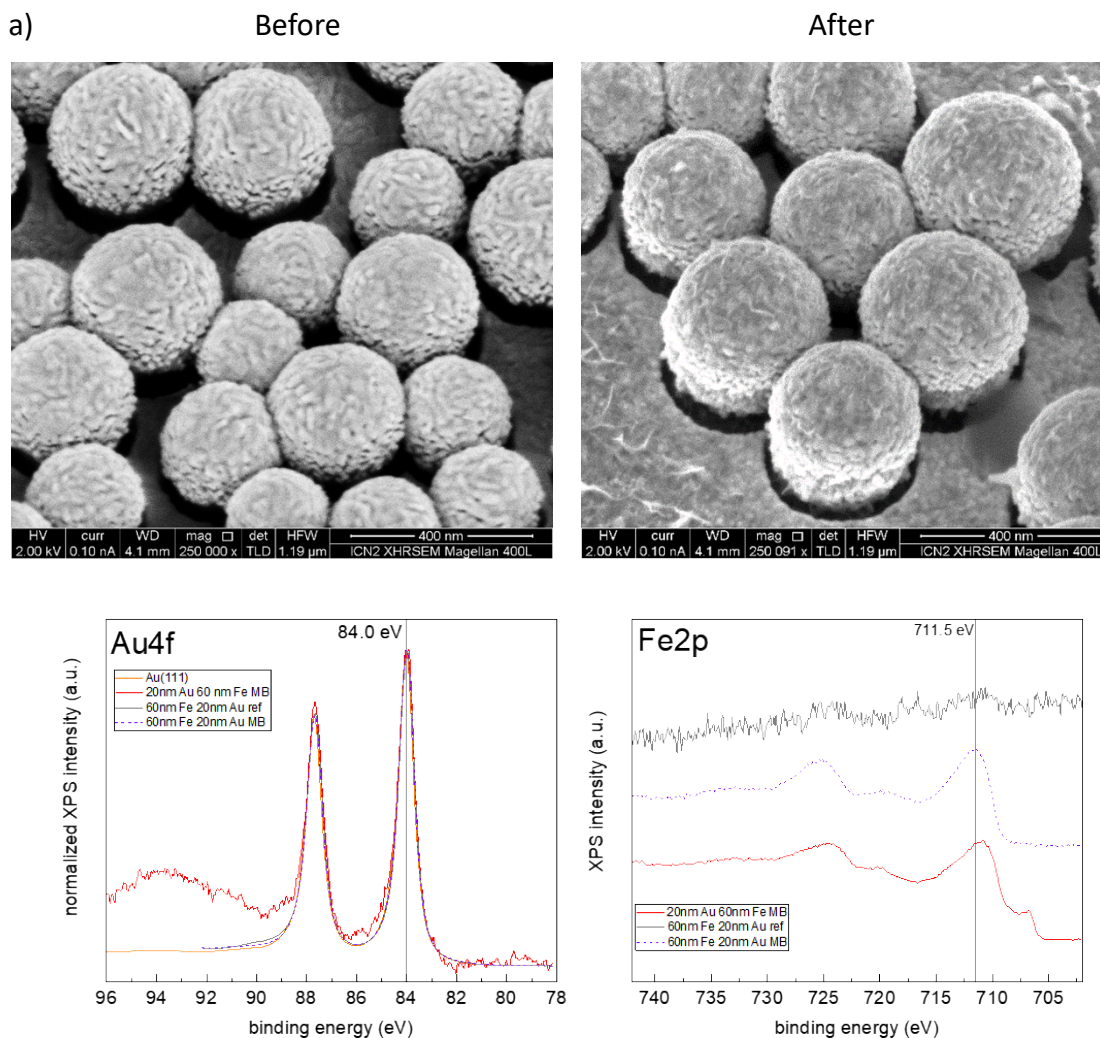


Figure. S7: a) SEM images of the Fe/Au GNCs before and after the 90 min reaction. b) XPS signal corresponding to Au and Fe for the following samples: Au monocrystal (Au 111), Au20nm/Fe60nm with Fe on top after the reaction (Au20 Fe60 MB), Fe60nm/Au20nm with Au on top before reaction (Fe60 Au20 ref) and after reaction with MB (Fe60 Au20 MB).

6. Catalytic activity tests

The catalytic performance of the Fe/Au GNCs was tested by analyzing the degradation and mineralization of two organic pollutants, Methylene Blue (MB) and Tetracycline (TC). For the degradation assays the evolution of the absorbance of MB and TC was analyzed, following the absorption peaks located at 664 and 362 nm, respectively. In these tests, the Fe and Fe/Au nanostructured catalytic surfaces deposited onto the silicon substrates (size 0.7x2 cm²) were immersed in the pollutant solution with initial concentrations of 3.2 mg/mL MB or 17.7 mg/mL TC at room temperature (25 °C). The color change and decrease of the absorbance were monitored in 15 min intervals using UV-vis spectroscopy (Cary 4000, PerkinElmer) in quartz-cuvettes. The degradation percentage (D%) of the pollutants was calculated by the following expression: $D\% = 100 \times (A_0 - A_t) / A_0$, where A_0 is the initial pollutant absorbance and A_t the pollutant absorbance at the final time point.

Total Organic Carbon Content (TOC) was used to evaluate the mineralization efficiency and confirm the degradation of the contaminants using TOC-VCSH equipment (Shimadzu) with a high-sensitivity column.

The catalytic tests were conducted in the presence of the oxygen naturally dissolved in water by the simple contact with atmospheric air.

To determine the influence of the Fe and Au thickness in the reactivity, MB degradation tests for the following configurations were carried out: Fe 20 nm / Au 20 nm; Fe 40 nm / Au 20 nm; Fe 60 nm / Au 20 nm, and Fe 60 nm / Au 10 nm (Figs. S8 a and b). These assays showed a significant decrease in the degradation efficiency when either the Fe or the Au layers thickness were reduced. In addition, the effect of the Fe and Au layers position was also analyzed, showing that the degradation efficiency dropped when the Fe layer was deposited on top of the Au layer due to the fast passivation of the Fe surface.

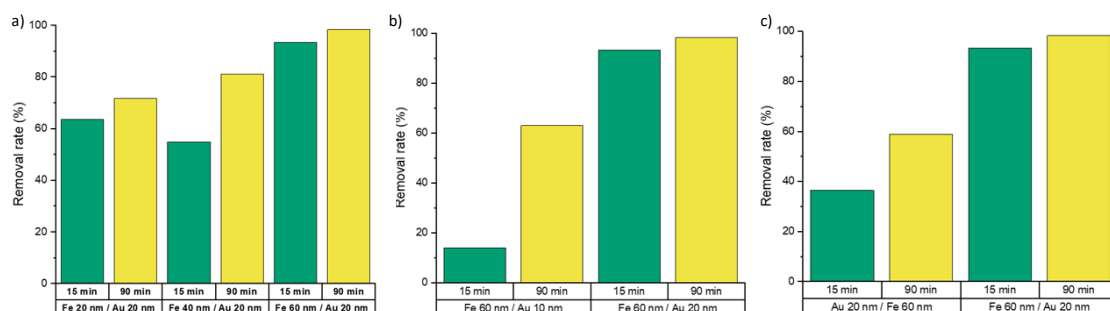


Figure S8. MB degradation rates for samples with different thickness and position of the Fe and Au layers. a) Degradation rates for Fe/Au layers with different Fe thickness. b) Degradation rates for Fe/Au layers with different Au thickness. c) Degradation rates for Fe/Au (Au on top) and Au/Fe (Fe on top) configurations.

To better assess the influence of dissolved oxygen in water, additional experiments were carried out in an argon (Ar) atmosphere using a glove box (Fig. S9).

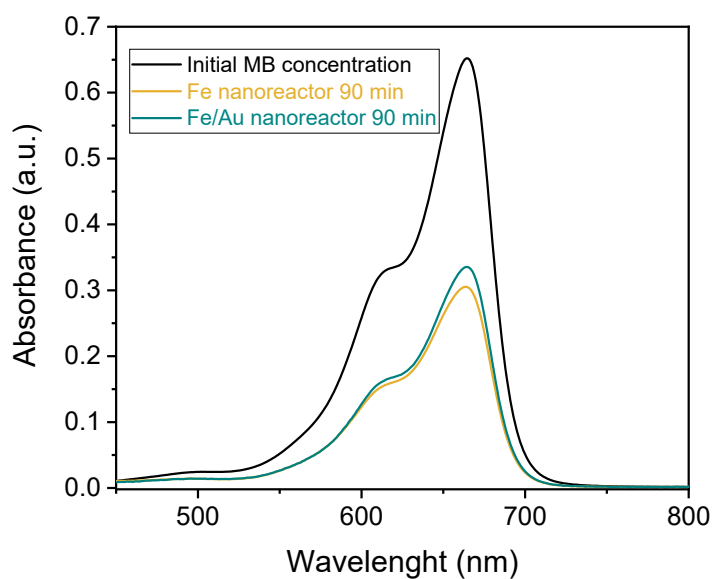


Figure S9. Absorbance measurements of MB before undergoing degradation and after interacting with Fe and Fe/Au nanostructures for 90 minutes in Ar atmosphere.

7. Scavenger experiments

Radical scavenging tests were carried out with the addition of scavenging agents in the MB solutions to identify the reactive oxygen species involved in the pollutant degradation. Accordingly, two different scavengers were used in presence of MB: benzoquinone (1 mM) as quencher of the superoxide radical ($\bullet\text{O}_2^-$), and isopropanol (1 mM) as a quencher of the hydroxyl radical ($\bullet\text{OH}$).